www.ietdl.org

Published in IET Microwaves, Antennas & Propagation
Received on 16th September 2009
Revised on 7th September 2010
doi: 10.1049/iet-map.2010.0016

ISSN 1751-8725

Rational interpolation scheme based on Bayesian classifiers for multi-resonance response of radio frequency devices

Y. El-Kahlout[1] *G. Kiziltas*[2]

[1]*Electrical and Electronic Eng., Istanbul Aydin University, Sefakoy 34295, Kucukcekmece, Istanbul, Turkey*
[2]*Mechtronics Program, Sabanci University, Orhanli 34956, Tuzla, Istanbul, Turkey*
E-mail: yasser@aydin.edu.tr

Abstract: Formal design optimisation techniques are commonly used for designing new radio frequency devices. The search for globally optimum designs turns out to be exhaustive primarily since full-wave electromagnetic (EM) simulation tools used in the repetitive analysis process during the design cycle consume plenty of time and resources. In this study, a new technique is introduced in order to reduce the number of analysis calls in a frequency-dependent EM optimisation cycle by providing a robust interpolation of the EM frequency response. The proposed technique makes use of Bayes' theorem incorporated with both rational interpolations and an adaptive sampling technique. The technique is tested on approximating the return loss curves of ten design candidates of a microstrip patch antenna. Results are compared with linear interpolation scheme demonstrating the technique's capability of accurately predicting poles and approximating resonance-based behaviour such as bandwidth with improved accuracy.

1 Introduction

Electromagnetic (EM) designs resulting from global design optimisation studies that allow for full design space exploration such as antenna shape, size, feed location and material distribution are expected to lead to novel configurations with enhanced performance such as in topology optimisation examples presented earlier [1, 2]. However, global synthesis via heuristic search techniques relies on considerable number of reanalysis calls which becomes a bottleneck in large-scale EM search studies where the objective function is a function of frequency and requires a new analysis per frequency. Hence, the computational time of analysis calls of the EM response, such as return loss curve, is proportional to the number of frequency points needed for predicting the EM response over the desired working frequency range. To address this issue, an approximation scheme suitable for approximating the frequency response of EM systems that will allow for fewer number and accurate reanalysis calls is developed in this paper. The interpolation problem becomes more challenging when the EM frequency response involves multiple resonances, as shown in Fig. 1, in the working range of interest, as typically encountered in concurrent conductor and material design studies of novel antennas [3, 4]. This in turn requires a robust adaptive sampling technique that ensures catching resonances while still keeping minimum number of frequency sampling points (support points).

Surrogate modelling techniques [5] are approximation schemes typically used for efficient EM reanalysis and serve a common central purpose by providing a 'virtual' objective function which can be called by the optimisation solver within a design cycle. Variations in the surrogate models are owing to training and/or tuning parameters. However, training a model of increased topological complexity leads to an excessive computational effort and most of the time results in a model that is problem dependent and the objective function in an optimisation process is only valid in a constrained sub-domain which is likely to contain the optimum.

Basis functions employed within the interpolation models have great influence on the quality of the surface approximation. Among alternatives, rational functions offer an attractive solution for providing approximate resonances because of their inherent pole predicting behaviour. Hence, their use has resulted in various representations of resonance-type responses with reasonable number of support points [6].

The rational-based approximation scheme proposed in this paper employs a simple and easy-to-train decision-making classifier based on Bayes' theorem to predict multi-resonance return loss curves of EM devices with complex topologies. Bayes' theorem has been extensively utilised for interpolation in signal processing problems [7, 8]. Similarly, the Bayesian classifier was used for predicting antenna frequency responses by determining a parameter of the interpolator basis function based on statistical assumptions

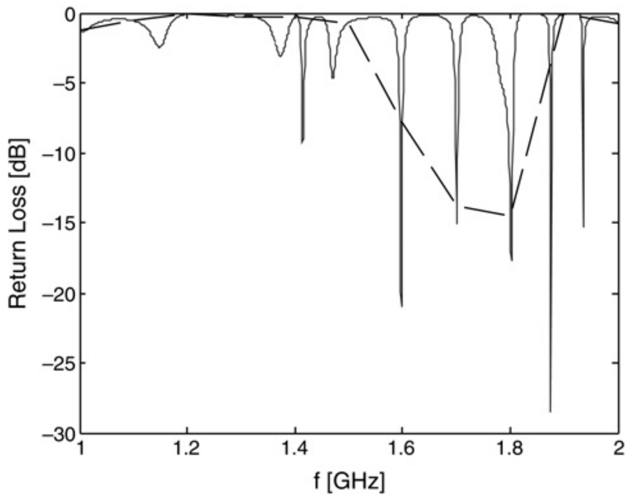

Fig. 1 *Return loss response of a microstrip patch antenna with multiple sharp resonances in a [1 2] GHz working frequency range linearly interpolated with 1001 and 11 uniform samplings (solid and dashed lines, respectively)*

[9]. This parameter, determined by the classifier 'coef' introduced in Section 2, controls the shape of the resulting resonances associated with a rational interpolator of quadratic numerator and denominator. The remaining rational function parameters are determined by known conditions of the interval of interest which are calculated using a finite-element-based analysis tool [10].

Selection of support points adaptively is known to affect the interpolation quality. Nevertheless, most adaptive sampling schemes available are suitable for global curve fittings that, unlike the proposed piecewise rational function, interpolate the whole range with a single interpolator [11, 12]. In this paper, the Bayesian-based rational interpolation (BRI) scheme proposed in [4, 9] is improved by employing the Bayesian classifier for adaptively sampling the frequency range via bisecting and hence refining the interval under consideration. The Bayesian trained rational function proves to have a powerful yet, unlike other standard approaches such as Neural Networks, simple approximation capability based on statistics and just a single controlling parameter. An in-depth analysis of the proposed Bayesian-based rational interpolation with adaptive sampling (BRIA) scheme is given in the next section and is followed by applying the proposed scheme to a large-scale design example where both the dielectric and conductor topologies are sought for a miniaturised novel antenna with broadband behaviour. Finally, the efficiency and reliability of the proposed scheme is discussed in the last section.

2 Interpolation method: Bayesian trained quadratic rational functions

In this section, the theoretical background of the rational function interpolation scheme based on the Bayesian classifier is presented. The numerator and denominator of the selected rational function are polynomials of second order. The order of the denominator is chosen to closely follow the behaviour of the return loss curve by allowing for a pole existence that emulates a resonance for each interval. To ensure smooth interpolations of successive intervals for a multi-resonance response curve, function values and first-order derivatives are imposed as constraints at the interval endpoints. The general form of the rational function is given as

$$y = \frac{\beta_1 + \beta_2 x + \beta_3 x^2}{1 + \beta_4 x + \beta_5 x^2} \tag{1}$$

where the coefficients $\beta_1 \ldots \beta_5$ are solved in order to satisfy four conditions at the endpoints of the interval of interest. Here, instead of following the standard approach to determine the remaining fifth coefficient, a heuristic-based approach is followed by employing Bayes' theorem such that the control of a possible existence of a pole inside the interval is possible. For mathematical convenience, the parameter β_5 is linked to the parameter β_4 by the following relation

$$\beta_5 = \frac{\text{coef}}{4}\beta_4^2 \tag{2}$$

The denominator of (1) now reads $1 + \beta_4 x + (\text{coef}/4)\beta_4^2 x^2$ and the roots are $r_{1,2} = \beta_4((-1 \pm \sqrt{1 - \text{coef}})/2)$. This relation yields a new parameter coef, which essentially replaces β_5, and can be tuned such that the rational function possesses a pole (a resonance) by enforcing the real part of the denominator root to lie inside the interval of interest. In addition, it is responsible for creating an imaginary part of the pole (when coef $\succ 1$) that in turn determines the sharpness of the resonance as will be discussed later. In a normalised interval with endpoints $x_0 = 0$ and $x_1 = 1$, the conditions to be satisfied are given by $y(0) = y_0$, $y'(0) = y'_0$, $y(1) = y_1$, $y'(1) = y'_1$.

Satisfying these conditions using (1) and (2), the coefficients $\beta_1 \ldots \beta_4$ are analytically determined as

$$\begin{aligned} \beta_1 &= y_0 \\ \beta_4 &= \frac{-b \pm \sqrt{b^2 - 4ac}}{2a} \\ \beta_2 &= y'_0 + y_0\beta_4 \\ \beta_3 &= y_1\left(1 + \beta_4 + \frac{\text{coef}}{4}\beta_4^2\right) - \beta_1 - \beta_2 \end{aligned} \tag{3}$$

where

$$\begin{cases} a = -\dfrac{\text{coef}}{4} y'_1 \\ b = y_1 - y_0 - y'_1 \\ c = 2(y_1 - y_0) - (y'_1 + y'_0) \end{cases}$$

Complex value solutions for these coefficients are allowed as they still yield real values for function and derivatives at endpoints and hence do satisfy the imposed endpoints conditions. The poles of the rational function are determined by the roots of the denominator, and therefore result in singularities in the form of sharp resonances. Moreover, certain function characteristics can be easily deferred based on the characteristics of the root r of the denominator. If the real part of r attains a value between 0 and 1, that is, falls inside the normalised interval, then the rational function naturally possesses a pole inside the interval of interest. Whenever the function variable x equals the real part of the complex pole r, the denominator

doi: 10.1049/iet-map.2010.0016

approaches a minimum value without changing sign. Hence, the rational function is highly likely to attain a resonance since this x value with a zero imaginary part is the closest to the complex root. If the interval contains a resonance, complex roots are desired since they prevent the denominator from changing sign and consequently enforce occurrence of single-peak poles as opposed to double-peak poles observed in the case of real-valued roots. Although a possible remedy to the sign change problem of the real root is to take the negative of the norm (in the case of return loss curves), these poles are still associated with singularities which physically correspond to the existence of very sharp resonances attaining infinite values and are not common in EM responses of practical devices. Therefore the selection of the parameter coef plays a significant role in determining three important behaviour characteristics:

1. the existence of the root inside the normalised interval;
2. the data type of the root (complex against real);
3. the imaginary to real part ratio of the complex root that controls the sharpness of the resonance.

The effect of the parameter coef on the resulting interpolation response function is depicted in Fig. 2. It is observed that as the value of coef changes, the behaviour of the resulting fitted curve represented by the dashed lines changes significantly from one with two sharp resonances near the interval endpoints (dashed line) to other approaching the original response (dash-dotted line).

Using the rational function in (2) and the β coefficient descriptions in (3), the roots of the denominator of the rational function given by (1) can be represented in terms of coef, y_1', b and c as shown in (4). Since the objective is to solve the inverse problem, that is, assign the root a certain value, (4) is solved for coef which is a non-linear relation and hence requires suitable iterative solvers such as Newton–Raphson, Levenberg–Marquardt etc. The parameters sgn_1 and sgn_2 can be either positive or negative and hence their sign combinations give rise to four different root possibilities given by (4). The roots $r_{1,2}$ are assigned to each endpoint of the scaled interval [0 1] and the resulting coefficients coef_1 and coef_2 refer to the left and right endpoints with $r = 0$ and $r = 1$, respectively. These are responsible for attaining real roots at the endpoints. Among possible solutions for coef_1s and coef_2s, the chosen solution set is the one within the range (coef_1 coef_2) that does not

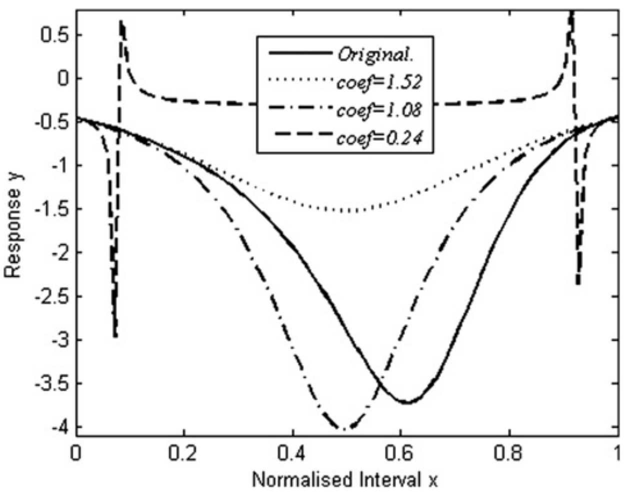

Fig. 2 *Effect of parameter coef on the interpolation response*

allow for a coef solution at the endpoints and hence a real root inside the interval is not allowed. Moreover, complex root findings are ensured by satisfying the condition coef $\succ 1$ as can be easily shown using (4).

$$r_{1,2} = \frac{b}{c\,\mathrm{coef}} - \frac{\mathrm{sgn}_1\,\mathrm{sgn}_2\sqrt{1-\mathrm{coef}}\sqrt{b^2+\mathrm{coef}\,y'c^2}}{c\,\mathrm{coef}} + \frac{\mathrm{sgn}_1\sqrt{b^2+\mathrm{coef}\,y'c^2}}{c\,\mathrm{coef}}\frac{b\,\mathrm{sgn}_2\sqrt{1-\mathrm{coef}}}{c\,\mathrm{coef}} \tag{4}$$

If the original data between the support points are not available (which is the case for a typical real interpolation process), tuning the parameter coef to closely follow the response is not possible. This problem can be overcome by heuristically determining the optimum value for the parameter coef using the Bayesian classifier [13]. For this, a training set with optimum coef values is prepared to train the classifier. The curves of the training set are finely sampled so as to obtain curves that can be considered exact/original and the optimum coef values are found using brute-force calculations by sweeping intervals (coef_1 coef_2) with small increments in order to minimise the root mean square error between the approximate interpolation and original response. A brute-force search instead of a more formal technique such as Golden Search or Fibonacci is followed since the function evaluations are considerably fast; search space is one-dimensional and bounded by (coef_1 coef_2); and the objective function to be minimised is not explicitly available in terms of the design variables making gradient-based techniques difficult to implement.

In d-dimensions the generate multivariate normal probability density function can be written as

$$p(\boldsymbol{x}) = \frac{1}{(2\pi)^{d/2}|\boldsymbol{\Sigma}|^{1/2}}\exp\left(-\frac{1}{2}(\boldsymbol{x}-\boldsymbol{\mu})^{\mathrm{T}}\boldsymbol{\Sigma}^{-1}(\boldsymbol{x}-\boldsymbol{\mu})\right) \tag{5}$$

where $\boldsymbol{x}$ is the attribute's variable vector and corresponds in this problem to the boundary conditions, $\boldsymbol{\mu}$ and $\boldsymbol{\Sigma}$ are the mean vector and covariance matrix of the training set, respectively, and d refers to the dimension of the problem. The coef parameter to be assigned to the interval is appointed to the class with maximum likelihood.

Since adaptive selection of support points is known to affect the interpolation quality, an adaptive procedure is employed here that allows for selecting support points by bisecting the interval of interest. This, although restricted to only bisecting the interval under consideration, allows for non-uniform sampling and hence creation of uneven interval lengths. Therefore another classifier 'bisect', utilising the same attributes used in the 'coef' classifier as described above is defined for producing an adaptive scheme. The bisect classifier is trained using the same training set used for training the 'coef' classifier and the data are obtained by giving the decision bisect or do not bisect according to the root mean square between the original and the approximate curves associated with the best coef found earlier for that interval.

Since only conditions at the interval endpoints are available to predict the response behaviour inside the interval, the attribute likelihoods are highly overlapping which results in a more difficult classification problem. The overlapping problem can be observed by investigating the likelihood distribution of both classes of the 'bisect' classifier against one attribute. Several improvements are performed on the

doi: 10.1049/iet-map.2010.0016

attributes in order to separate their likelihoods and enhance the classification results. First, the training data of each attribute for the coef Bayesian classifier are scaled with respect to the mean value. In addition to the conditions at the interval endpoints, attributes such as interval length or a combination of attributes are also considered in order to enhance the training process. Finally, the occurrence of positive and negative slopes at the boundaries is taken into account by considering the norm of the attributes leading to a better training performance. This improvement is linked to the symmetry characteristics of an interval containing a resonance, and hence, it inspires the use of a new attribute in the form of the product of the maximum of slope norms at the interval endpoints and the length of the interval, that is, $|y'_{\max}|\Delta x$. The maximum slope at the interval endpoints and the length of the interval are proportional to the likelihood of this interval containing a resonance.

It is finally noted that the conductor and material topologies are random by nature within topology optimisation studies; and parameters coef and bisect for such design efforts are trained based on such random antenna structures. Hence, this training parameter pair has the capacity to represent a very wide class of antenna structures (such as any probe fed radiating printed conductor topology (E-shaped, spiral, patch etc.) as long as the finite element analysis (FEA) discretisation allows. Same applies to the supporting dielectric material substrate. It can be homogeneous, multi-layered, layered with inclusions etc. and the already trained set can be used for a wide range of antenna structures. On an additional note, the training effort is truly simple and quick enough and demands very little computational time so that new trainings can be conducted easily for each new design problem.

3 Design example

In this section, the proposed BRIA scheme is applied to approximate the return loss curves of microstrip antennas with complex topological structures. The complex topology is a result of aiming to design both the supporting dielectric material substrate and the radiating patch from scratch for optimal performance. More specifically, novel antenna structures are designed from scratch by distributing various shades of off-the-shelf ceramics with different permittivities into the discrete design cells of the volume that the dielectric substrate will occupy and by assigning discrete surface design cells with void or solid conductors as shown in Fig. 3. This complex antenna topology is expected to result in a complex return loss response curve with multi-resonances as shown by the solid line in Fig. 1. More specifically, within topology optimisation problems where one essentially searches for the optimum among random conductor and material topologies (constrained by FEA surface discretisation), it is highly likely that many of them are irregular conductors and material substrates, and hence are indeed multi-resonance cases unless restricted intentionally. Hence, the approximation that will result via the proposed scheme can be used in a large-scale heuristic/global-based optimisation process such as topology optimisation in order to find the optimum conductor patch and material distribution of the substrate that maximises antenna bandwidth subject to given size requirements. More specifically, the objective in the chosen design example is to maximise bandwidth, and therefore the interpolation scheme has to predict the bandwidth of the antennas with complex topologies. Similar challenging design problems were presented earlier [1].

Part of the design domain comprises the volumetric space that the dielectric material of the antenna substrate occupies. It is 0.3715 cm thick and covers a surface area of 2.5 cm × 2.5 cm. Remaining design domain belongs to the printed surface conductor and comprises the entire top surface of the substrate. The substrate is discretised into $2 \times 20 \times 20 = 800$ triangular-prism-shaped finite elements. A design cell is considered to be a square prism composed of two adjacent triangular finite-element prisms and therefore reduces to a total of 400 design cells. The permittivity of each volumetric design cell is taken as a material design variable. The design domain for the conductor is similarly discretised into $2 \times 20 \times 20 = 800$ triangular finite-element cells corresponding to a total of 400 square conductor design cells. Each design cell is essentially a design variable of on/off type representing the presence or absence of conductor material in that specified design cell.

The training data set of the classifier belongs to return loss responses of microstrip antennas as depicted schematically in Fig. 3 with random topologies obtained during the evolution

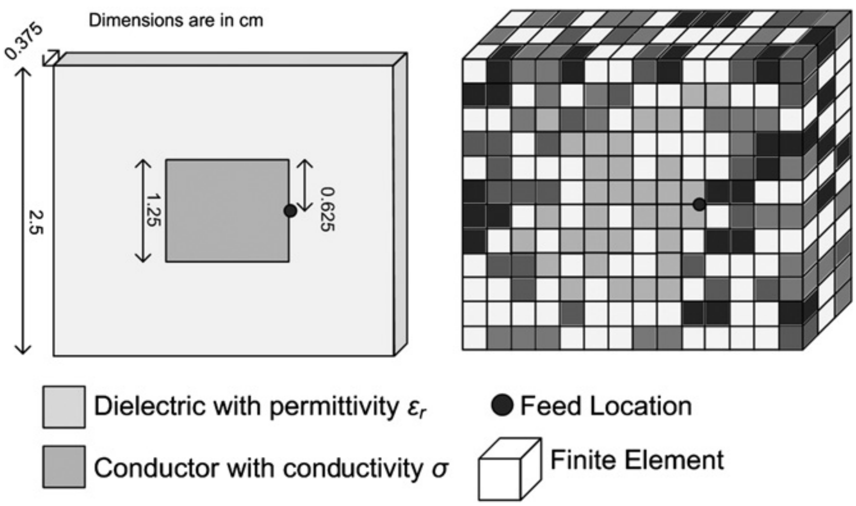

Fig. 3 *Patch antenna on left is supported by homogeneous substrate where the antenna on right has arbitrary patch (grey) and material distribution (colour)*

doi: 10.1049/iet-map.2010.0016

of a topology optimisation problem. In a possible optimisation scenario of the large-scale design problem, the optimiser will call for multiple reanalysis of the full-wave bandwidth response in a frequency range of [1 2] GHz. In order to accurately predict the return loss response used for calculating the fitness function represented by the bandwidth, normally a frequency sampling with 10 MHz intervals is needed. The return loss curve of a representative microstrip antenna with complex conductor coating and multi-material substrate topology is depicted in Fig. 1. The dashed line response is clearly a wrong prediction of the return loss curve that would lead to an intolerably wrong fitness value of the candidate individual's bandwidth because of insufficient frequency sampling. Moreover, a small error of around 5% which may be acceptable for practical purposes could cause divergence within design studies of complex antenna designs. More specifically, miscalculated responses such as in Fig. 1 will mislead the optimiser during the search since optimisation methods whether heuristic or gradient based locate the optimum by using information from previous iterations or generations and their convergence performance depends heavily on regions/individuals with promising design candidates. This effect becomes more pronounced as small variations in the topology of the device may cause drastic changes in the response while searching within an extremely large design domain of topology optimisation methods. Therefore reliable predictions with as much accuracy as possible is needed from the interpolation scheme within antenna design search studies where the topology can vary significantly and the performance is highly likely to be a multi-resonate one with possible sharp multiple resonances.

The analysis tool used in generating simulated bandwidth response data is a finite-element boundary integral model based on a fast spectral domain algorithm [1, 14]. Topology optimisation is a design approach that relies on optimisation techniques while searching for the optimal material distribution of a device. The computational time to reach convergence for the design algorithm where each design cell is treated as a design variable and the antenna performance is reanalysed at each iteration for multiple frequencies would correspond to impractical timespans. The reason why topology optimisation even if linked to gradient-based optimisers (which despite the derivative information could be very efficiently calculated through the use of the adjoint variable method) is time consuming is again because of the bottleneck being computational cost of the full-wave analysis of complex antennas and the need to sample highly over the desired frequency range.

The proposed Bayesian-based rational fitting scheme is integrated to the full-wave simulator in order to interpolate the return loss response over a 1–2 GHz frequency range with a frequency sweep according to the proposed adaptive scheme using the 'bisect' classifier. The results of the interpolation scheme are presented in the next section.

4 Results

The resulting rational interpolation response relies on the use of first-order derivative values at sampled support points. These are computed numerically with 1% variable perturbation via forward finite differences. To isolate the effect of gradient calculations on the computational savings via interpolations, Bayesian-based interpolation results are compared with both naïve linear interpolation (LI) and LI using double number of support points (LIDS). The latter is representative for the case of forward difference-based rational interpolation. The error norm for comparing resulting interpolations in terms of accuracy is chosen as the bandwidth error calculated at −5 dB between interpolated and original return loss values. Original curves are LIs with 1 MHz frequency samplings, that is, 1001 support points exist between 1–2 GHz. A total of 200 sub-intervals associated with known boundary conditions (support point values and their first derivatives) and known-interval lengths belong to return loss curves of ten different design candidates with different material and conductor topologies similar to that in Fig. 2. It is noted that all of these design curves have multi-resonances with nine out of these ten designs exhibiting at least two resonances below −5 dB. These sub-intervals were used in training the Bayesian classifier to predict the optimum parameter coef and to adaptively sample at informative support points. Fig. 4 depicts a comparative interpolation study for one of the ten return loss curves. Specifically, results are shown for interpolations obtained using the proposed BRIA scheme, BRI scheme using uniform sampling, LI using uniform sampling with the same number of support points obtained

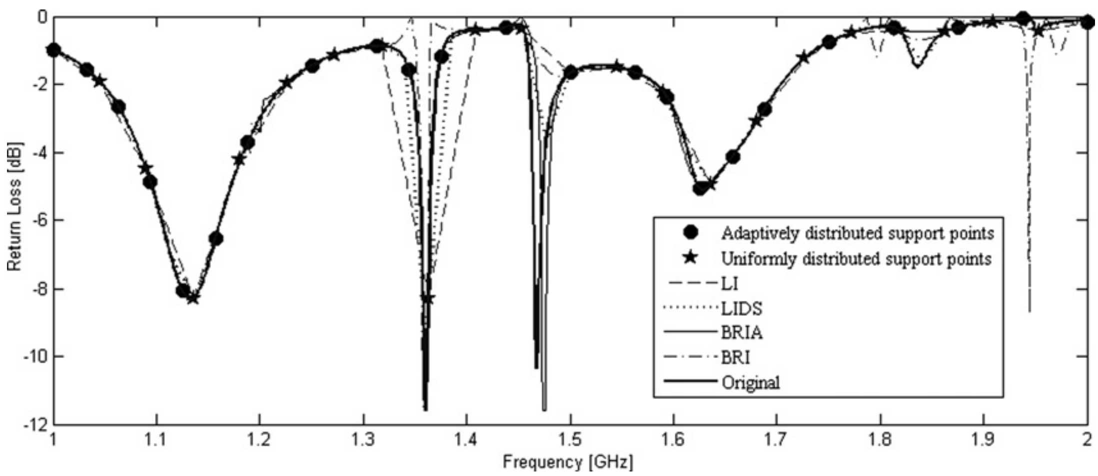

Fig. 4 *Return loss curve interpolations of a microstrip patch antenna design (see Fig. 3) using naïve LIs with regular uniformly distributed support points (LI) and LIDS, BRI with uniform sampling and (BRIA)*

doi: 10.1049/iet-map.2010.0016

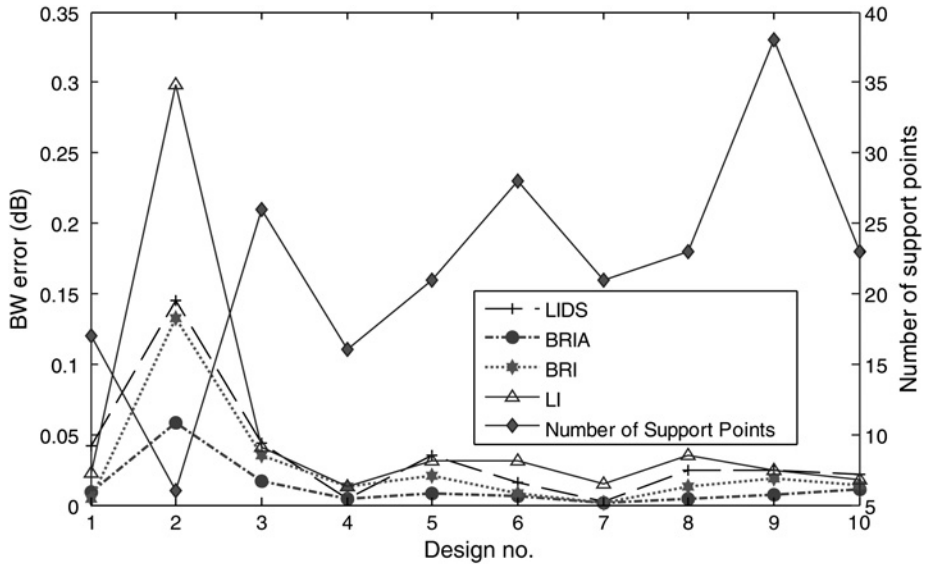

Fig. 5 *Interpolation error (bandwidth difference) of LIs, LIDS, BRIA and BRI for ten different designs and the total number of support points used in all schemes*

in BRIA, and LIDS with uniform sampled double number of support points. The latter interpolation is presented in order to account for the extra computational effort used in calculating the derivatives of the proposed BRIA and BRI schemes. As the results show, treating resonances with s_{11} values < -5 dB as significant, the bandwidths of all four major resonances are more accurately predicted by the BRIA than any other interpolation scheme. It is noted that 'glitches' such as the one around 1.94 GHz in the BRI curve result from the nature of rational functions. More specifically, owing to the presence of a denominator of a second order, if the pole happens to be inside the interval then a very narrow dip/glitch can occur in the interpolation. Care was taken while preparing the training set in order to minimise this undesired behaviour. Nevertheless, a small classification error can still result in producing these glitches. As a possible extension of the proposed method, a remedy could be to restrict the classification from attaining these undesired glitches by characterising the resulting coef value and restricting it from producing a real root in the denominator. This strategy, however, would increase the complexity of the interpolation process.

Fig. 5 compares the bandwidth error of the approximated responses belonging to the ten antenna designs with respect to all four interpolation schemes with equal number of support points as used in the BRIA scheme. Based on these results, the BRIA strategy shows an improvement via use of the 'coef' and 'bisect' classifiers by decreasing the average bandwidth (BW) error (of the ten design cases) by 74.12, 60.59 and 44.11% when compared with the LI, LIDS and BRI schemes, respectively. Despite the existence of rare cases where BRIA is very close to the accuracy performance of the LIDS (such as in designs 4, 5 and 8), overall error of the BRIA method consistently remains below an error threshold that is half of that in LIDS and one-fifth of that in LI. Additionally, there is another robustness aspect of BRIA where it outperforms standard schemes including LIDS and needs to be considered in addition to its overall accuracy advantage. Design cases with relatively closer Bayesian-based interpolation errors to LIDS are re-examined and a representative interval of a single resonance out of the many possible is displayed in Fig. 6. Although the centre plot (Fig. 6*b*) is in favour of the double sampled LI, perturbation of support points to the left or to the right (Figs. 6*a* and *c*, respectively) reveals that LI (with double number of support points in this case) is more viable to the location of support points than the Bayesian-based rational fitting that consistently predicts the pole and approximates the bandwidth with better accuracy. This behaviour is consistently observed for all other design cases and is a clear indication of the latter being more robust to uniformly distributed support points than naïve LI.

Fig. 5 also depicts the total number of support points used in each design case that is determined by the adaptive scheme

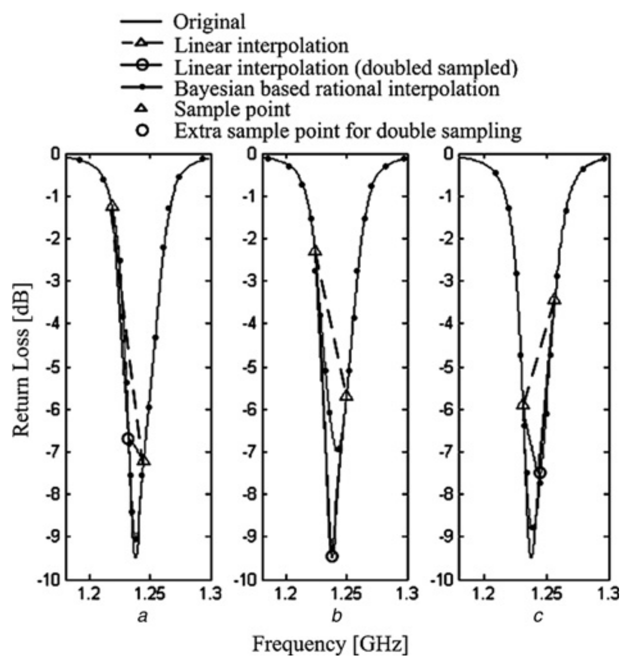

Fig. 6 *Effect of frequency sampling perturbation on rational interpolation LI, and LI using double-support points*

a Perturbed to the left interval [1.220 1.245]
b Initial interval [1.224 1.249]
c Perturbed to the right [1.300 1.325]

of BRIA. However, the computational time is not cited in terms of absolute time but rather the number of sample points is given since the major contribution to the total computational time of the interpolation within the reanalysis amounts to repetitive calls to the full-wave analysis and is directly proportional to the number of samples over the frequency range which is the same for the Bayesian-based and LI technique. More specifically, the total computational cost for either interpolation technique in its most general case has four components:

1. time required for the full-wave analysis simulations to compute y_0 and y_1 values;
2. time required for the full-wave analysis simulations to compute y'_0 and y'_1 derivative values using the finite-difference method;
3. training time to train parameters coef and/or bisect;
4. time required to compute interpolation parameters such as the coefficients and $p(x)$ function in (3) and (5), respectively.

Second and third components are specific to the Bayesian method whereas first and final components are common in both interpolations with the fourth component depending on the interpolation method.

The computational cost of training the Bayesian classifier for the example chosen is 0.112 s and is performed only once; the parameter calculation time amounts to about $3e^{-6}$s against $3e^{-7}$s for Bayesian and LI, respectively, whereas a full-wave analysis for one frequency sample takes 1.5 min (and two sample calculations are needed for evaluating each derivative y'_0 and y'_1 using the finite-difference method). Consequently, the computational time of a real design process is predominantly controlled by the number of frequency points or support points. Therefore it is fair to say that in addition to the advantages of accuracy as shown in Fig. 5 and robustness characteristics as shown in Fig. 6, the BRIA method demands the training of only two parameters (coef and bisect) and quick evaluation of interpolation coefficients to arrive at the interpolation function within sub-seconds proving the method's power.

It is also noted that the BW error has an overall reverse trend to that of the number of support points. In average, 23 support points were required for approximating the response of an antenna with a complex topology.

5 Conclusion

This paper presented an interpolation scheme based on Bayesian trained quadratic rational functions with adaptive sampling, BRIA, for approximating frequency-based EM return loss responses. The scheme was proposed to be used within challenging design search studies where the search is time consuming and the designs are non-intuitive with random conductor and material topologies. Results indicate that this scheme is an efficient tool in predicting poles and characterising resonance-based behaviour such as bandwidth of RF devices. The application of the proposed strategy with adaptive sampling outperforms the same scheme without adaptive sampling (BRI), LI and LIDS as the error consistently remains below an error threshold that is half of that in LIDS and one-fifth of that in LI. In addition to the advantages of accuracy and robustness, the BRIA method demands the training of only two parameters and quick evaluation of interpolation coefficients. Hence, it is a powerful tool in providing efficient and simple reanalysis in large-scale design optimisation studies of novel EM devices such as the design of conductor and material topologies from scratch for novel antennas with enhanced performance.

6 Acknowledgments

This work was supported in part by Yousef Jameel PhD scholarship, TUBITAK grant 2215, TUBITAK Grant 106M348 and TUBA GEBIP award.

7 References

1 Kiziltas, G., Psychoudakis, D., Volakis, J.L., Kikuchi, N.: 'Topology design optimization of dielectric substrates for bandwidth improvement of a patch antenna', *IEEE Trans. Antennas Propag.*, 2003, **51**, pp. 2732–2743
2 Nomura, T., Sato, K., Taguchi, K., Kashiwa, T.: 'Topology optimization method for antenna design using FDTD Method', *IEICE Trans. Electron.*, 2006, **12**, pp. 2196–2205
3 Koulouridis, S., Psychoudakis, D., Volakis, J.L.: 'Multiobjective optimal antenna design based on volumetric material optimization', *IEEE Trans. Antennas Propag.*, 2007, **55**, pp. 594–603
4 El-Kahlout, Y., Kiziltas, G.: 'An efficient optimization framework for material and conductor designs of antennas'. Int. Conf. on Electromagnetics in Advanced Applications, Torino, Italy, 2007, pp. 555–558
5 Jones, D.R.: 'A taxonomy of global optimization methods based on response surfaces', *J. Glob. Optim.*, 2001, **21**, p. 345
6 Kottapalli, K., Sarkar, T.K., Hua, Y., Miller, E.K., Burke, G.J.: 'Accurate computation of wide-band response of electromagnetic systems utilizing narrow-band information', *IEEE Trans. Microw. Theory Tech.*, 1991, **39**, pp. 682–687
7 Yibin, Z., Doerschuk, P.C., Johnson, J.E.: 'Symmetry-constrained 3-D interpolation of viral X-ray crystallography data', *IEEE Trans. Signal Process.*, 2000, **48**, pp. 214–222
8 Fearnhead, P.: 'Exact Bayesian curve fitting and signal segmentation', *IEEE Trans. Signal Process.*, 2005, **53**, pp. 2160–2166
9 El-Kahlout, Y., Kiziltas, G.: 'Bayesian trained rational functions for electromagnetic design optimization'. IEEE Int. Symp. on Antennas and Propagation, Honolulu, Hawai'i, USA, 2007, pp. 3952–3955
10 Eibert, T.F., Volakis, J.L.: 'Fast spectral domain algorithm for hybrid finite element/boundary integral modelling of doubly periodic structures'. IEE Proc. Microwaves, Antennas and Propagation, 2000, pp. 329–334
11 Lehmensiek, R., Meyer, P.: 'Creating accurate multivariate rational interpolation models of microwave circuits by using efficient adaptive sampling to minimize the number of computational electromagnetic analyses', *IEEE Trans. Microw. Theory Tech.*, 2001, **49**, p. 12
12 El-Kahlout, Y., Kiziltas, G.: 'Global design optimization of complex electromagnetic devices via efficient frequency response interpolations'. IEEE Int. Symp. on Antennas and Propagation, San Diego, CA, USA, 2008, pp. 1–4
13 Han, J., Kamber, M.: 'Data mining: concepts and techniques' (Simo Fraser University, Morgan Kaufmann Publisher, 2001)
14 Erdemli, Y., Sertel, K., Gilbert, R.A., Wright, D.E., Volakis, J.: : 'Frequency selective surfaces to enhance performance of broadband reconfigurable arrays', *IEEE Trans. Antennas Propag.*, 2002, **50**, pp. 1716–1724

doi: 10.1049/iet-map.2010.0016